Available online at www.sciencedirect.com
SCIENCE DIRECT
International Journal of Heat and Mass Transfer 49 (2006) 3655–3669
International Journal of HEAT and MASS TRANSFER
www.elsevier.com/locate/ijhmt

Buoyancy driven vortex flow and its stability in mixed convection of air through a blocked horizontal flat duct heated from below

S.W. Chen, D.S. Shu, J.T. Lir, T.F. Lin *

Department of Mechanical Engineering, National Chiao Tung University, Hsinchu, Taiwan 30010, ROC

Received 11 July 2005; received in revised form 19 February 2006
Available online 18 April 2006

Abstract

Experimental flow visualization combined with transient temperature measurement are carried out here to explore the possible stabilization of the buoyancy drive vortex flow in mixed convection of air in a bottom heated horizontal flat duct by placing a rectangular solid block on the duct bottom. Two acrylic blocks having dimensions $40 \times 20 \times 5$ mm^3 (block A) and $40 \times 20 \times 10$ mm^3 (block B) are tested. The blocks are placed on the longitudinal centerline of the duct bottom at selected locations. How the location and orientation of the rectangular block affect the stability of the regular vortex flow is investigated in detail. Experiments are conducted for the Reynolds number varying from 3 to 30 and Rayleigh number from 3000 to 6000, covering a wide range of the buoyancy-to-inertia ratio. For longitudinal vortex flow, the presence of either block near the duct entry causes the onset points of the longitudinal rolls to move significantly upstream especially for the roll pair directly behind the block. Besides, the longitudinal vortex flow in the exit portion of the duct is destabilized by the block. The transverse vortex flow is found to be only slightly affected by the block when it is placed in the exit half of the duct. Significant deformation of the transverse rolls is noted as they pass over the block. However, they restore to their regular shape in a short distance. Substantial decay in the transient flow oscillation results in the region right behind the block. Elsewhere the flow oscillates at nearly the same frequency and amplitude as that in the unblocked duct. When the block is placed near the duct entry, stabilization of the vortex flow behind the block is more pronounced. This flow stabilization is more prominent for block B with its height being twice of block A. Placing the block with its long sides normal to the forced flow direction can also enhance the flow stabilization. For the mixed longitudinal and transverse vortex flow, placing the block near the duct inlet causes the transverse rolls to change to regular or deformed longitudinal rolls in the duct depending on the buoyancy-to-inertia ratio and orientation of the block. The flow stabilization by the block is substantial. Again the stabilization of the mixed vortex flow can be enhanced by increasing the block height and length and by placing the block with its long sides normal to the forced flow direction.

1. Introduction

Vortex flow in the form of steady regular longitudinal and time periodic downstream moving transverse rolls, and a mixture of both induced at slightly supercritical buoyancy in a mixed convective gas flow through a bottom heated horizontal flat duct has been known for some time and is well documented in the literature [1]. At buoyancy well above certain critical level unstable vortex flow appears and the vortex rolls become deformed and time dependent. At an even higher buoyancy irregular rolls prevail in the duct. The highly efficient heat transfer associated with the unstable vortex flow is most welcome by the technological applications such as cooling of microelectronic equipments [2] in which the efficient energy transport is of major concern. It is of interest to note that the microelectronic components on the printed circuit boards existing in the cooling channel for the microelectronic equipments can destabilize the coolant flow and hence can enhance the heat removing rate. Over the past, the use of various wall-mounted protrusions to promote the heat transfer has been extensively studied for both laminar

* Corresponding author. Tel.: +886 35 712121x55118; fax: +886 35 726440.
E-mail address: tflin@mail.nctu.edu.tw (T.F. Lin).

0017-9310/$ - see front matter © 2006 Elsevier Ltd. All rights reserved.
doi:10.1016/j.ijheatmasstransfer.2006.02.025

Nomenclature

A	aspect ratio, b/d
b, d, l	test section width, height, length
g	gravitational acceleration
Gr	Grashof number, $\beta g d^3(T_h - T_c)/\nu^2$
Gr/Re^2	buoyancy-to-inertia ratio
h	length of the mounted block
k	thermal conductivity
$P_1 \ldots P_6$	location of mounted block in the duct
Pr	Prandtl number, ν/α
Ra	Rayleigh number, $\beta g d^3(T_h - T_c)/\alpha\nu$
Re	Reynolds number, $W_m d/\nu$
t	time, s
t_p	period of flow oscillation
T	temperature
T_c	temperature of the top plate
T_h	temperature of the bottom plate
T_m	mean temperature, $(T_h + T_c)/2$
W_m	mean velocity component in z direction
x, y, z	dimensionless Cartesian coordinates all scaled with d
α	thermal diffusivity
β	thermal expansion coefficient
θ	dimensionless temperature, $(T - T_m)/(T_h - T_c)$
ν	kinematic viscosity

and turbulent flows. However, in the chemical vapor deposition (CVD) processes [3] used frequently to grow thin crystal films on silicon substrates, the presence of the vortex flow will result in a non-uniform chemical vapor deposition, producing a thin crystal film of non-uniform thickness. Moreover, the unstable vortex flow will provoke a time-dependent deposition rate. Both the stable and unstable vortex flows are not welcome and should be avoided in the CVD design. Simple means such as lowering the chamber pressure, which can effectively reduce the buoyancy effects [3], and accelerating the main gas flow through the substrate inclination have been adopted in real CVD processes to stabilize the vortex flow. But it is rather costly in reducing the chamber pressure. Besides, the substrate inclination is only good for stabilizing the temporal oscillations of the vortex flow [4]. It is not effective in wiping out the spatial structures of the vortex flow. Other methods need to be sought to stabilize the temporal flow oscillations and to suppress the spatial vortex structure in the mixed convective duct flow. In this experimental study we explore how the buoyancy driven vortex flow and its stability are affected by a rectangular solid block mounted on the bottom of a horizontal flat duct heated from below. In what follows the relevant literature on the mixed convective flow in horizontal blocked and unblocked flat ducts is briefly reviewed.

Previous studies on various aspects of the buoyancy induced vortex flow in an unblocked horizontal flat duct are reviewed first. In a long horizontal plane channel with the bottom plate at a higher uniform temperature than the top one by ΔT, the critical Rayleigh number for the onset of the vortex flow was found to be around 1708, as predicted from experimental measurements and linear stability theory [5,6]. Ostrach and Kamotani [7] and Kamotani and Ostrach [8] experimentally noted that the longitudinal vortex rolls appeared when the temperature difference became larger than a critical value corresponding to $Ra = 1708$. Above the critical point, the heat transfer rate is increased by the thermal instability and the temperature field is strongly influenced by the motion of the vortex flow. When $Ra > 8000$, the vortex rolls become irregular. Hwang and Liu [9] visualized the onset of secondary flow and showed that the wave number of vortex rolls remained constant along the flow direction. Experiments conducted by Incropera et al. [10] and Maughan and Incropera [11] disclosed four flow regimes along the bottom plate-laminar forced convection, laminar mixed convection, transitional mixed convection, and turbulent free convection. The transition to turbulent flow was attributed to the breakdown of vortices due to the hydrodynamic instability. Besides, a correlation for the onset point was proposed. Criteria for the onset of vortex instability and the start of the transition from two-dimensional laminar flow to three-dimensional vortex flow in mixed convective air flow over an isothermally heated horizontal flat plate were established by Moharreri et al. [12]. The vortex flow regime starts with a stable laminar flow region where vortices develop and grow gradually and ends with an unstable flow region where the vortices mix together and collapse to form a two-dimensional turbulent flow regime.

In the mixed convection of nitrogen gas between two horizontal, differentially heated parallel plates, Rosenberger and his colleagues [13,14] showed that the critical Ra for the appearance of the transverse convection rolls increased with Re. They also found that at a high Ra, the longitudinal rolls were unsteady and snaking. Besides, they showed the regime of Ra and Re leading to a steady or unsteady flow. Nyce et al. [15] showed the variations of velocity field in both axial and transverse directions which were consistent with the presence of both longitudinal roll and transverse wave instabilities. The transverse rolls were noted at a very low Reynolds number by Ouazzani et al. [16,17]. They also refined the regime map to include the transverse rolls. The recent flow visualization from Yu et al. [1] showed that at a fixed Ra but in reducing Re the vortex flow transformed from the structure prevailed by the longitudinal rolls to transverse rolls in sequence of stable longitudinal rolls, unstable longitudinal rolls, intermittent transitional vortex flow, mixed longitudinal and transverse rolls, and transverse rolls. Photographic results

from Cheng and Shi [18] revealed the convective instability and chaotic phenomena caused by the buoyancy forces. Koizumi and Hosokawa [19] presented the sidewall temperature profile in a horizontal rectangular duct heated from below, which simulated a horizontal thermal CVD reactor. They found that although the flow was unsteady but the time-averaged local mass transfer rate on the bottom wall can be almost uniform.

Fluid flow and heat transfer around a wall-mounted block in a channel have been extensively studied in recent years. Several different flow patterns are generated near the wall-mounted block such as horseshoe and corner vortexes, and these vortexes significantly augment the heat and mass transfer from the surface of the block. Chyu and Natarajan [20] experimentally showed that the mass transfer rate was high at the side surface and lowest at the rear surface around a wall-mounted cube at high Reynolds numbers. Igarashi [21] and Hsieh et al. [22] examined the heat transfer around a mounted rib and proposed the relations between the convection heat transfer coefficient and the Reynolds number of the flow and the aspect ratio of the duct. Besides, Igarashi [23] classified the flow patterns around a prism into four types and suggested the average maximum and minimum heat transfer coefficients for different angles of attack to an air stream. Moreover, Chyu and Natarajan [24] tested heat transfer for five different basic geometric blocks and suggested an inter-element spacing for array configurations based on the optimal heat transfer performance. In addition, the effective use of multiple wall-mounted ribs to enhance heat transfer in turbulent channel flow was demonstrated by Han et al. [25,26]. These studies focused mainly on the heated transfer augmentation by the mounted blocks. Very little is devoted to investigating the possible stabilization of the oscillating vortex flow driven at high buoyancy-to-inertia ratio by mounting a block in a duct.

The above literature review clearly reveals that there has been a substantial amount of research carried out in the past on various aspects of vortex flow and heat transfer in mixed convection of gas in a horizontal unblocked flat duct. Moreover, the use of blocks to enhance the heat transfer and the associated flow characteristics have been extensively studied for both laminar and turbulent flows. In the present study an experimental investigation is carried out to unravel how a wall-mounted rectangular protrusion affects the buoyancy induced vortex flow structure in the low Reynolds number mixed convection of air in a bottom heated horizontal flat duct. Attention will be focused on how the three regular vortex flow patterns, namely, the longitudinal, transverse and mixed vortex rolls, are influenced by the presence of the block in the channel. The effects of the block size and location in the channel on the vortex flow will be examined in detail. In the experiment the Reynolds number of the flow is varied from 3.0 to 30 and Rayleigh number from 3000 to 6000. Both the changes in the spatial and temporal structures of the vortex flows will be inspected carefully. It should be pointed out here that the vortex flow structures in mixed convection of air in a flat duct are closely related to the Nusselt number distribution on the duct bottom, according to our numerical computation [27]. Thus the information on the vortex flow characteristics is valuable in improving the design of CVD flow configurations.

2. Experimental apparatus and procedures

The experimental system established in the previous study [1] is used here to investigate how the buoyancy driven vortex flow is affected by a rectangular block mounted on the duct bottom in mixed convective air flow through a horizontal flat duct heated from below.

2.1. Experimental apparatus

The experimental apparatus is schematically shown in Fig. 1. The open-loop mixed convection apparatus consists of three parts: wind tunnel, test section, and measuring bench for the velocity and temperature, which is connected with a data acquisition unit.

The test section is a rectangular duct of 240-mm wide and 300-mm long with the duct height of 20-mm between the top and bottom walls, providing an aspect ratio of $A = 12$. The bottom plate of the test section is made of a 15-mm thick, high purity copper plate and is electrically heated by DC power supplies. The top plate of the test section is made of a 3-mm thick glass plate and a 2-mm thick plexiglass plate with a gap width of 3-mm. This top plate is reinforced by copper alloy frames to keep it flat. Distilled water is provided from a constant temperature circulation unit and flows into this gap to control the upper plate temperature.

The working fluid is air which is driven into the system by a 7.5-hp air compressor and sent into a 300-l high pressure air tank. The air is first regulated by a pressure regulator and then passes through a settling chamber, a contraction nozzle, a developing section, the test section, and finally discharges into the ambient surrounding. The developing section is 1690-mm in length, approximately 84 times of the duct height. This insures the flow being fully developed at the inlet of the test section for $Re < 50$. An outlet section of 190-mm long is added to the test section to reduce the effects of the disturbances from discharging the flow to the ambient surrounding of the open-loop wind tunnel.

The volume flow rate of air is controlled and measured by two Hasting HFC flow controllers designed especially for low volume flow rates, with accuracy better than 1%. A thermocouple probe, which is an OMEGA (model HYP-O) mini hypodermic extremely small T-type thermocouple (33 gauge) implanted in a 1 in. long stainless steel hypodermic needle, supported by a three-way traversing stand is used to measure the instantaneous air temperature in the test section. In order to unravel the unsteady thermal characteristics of the vortex flow, the transient temperature

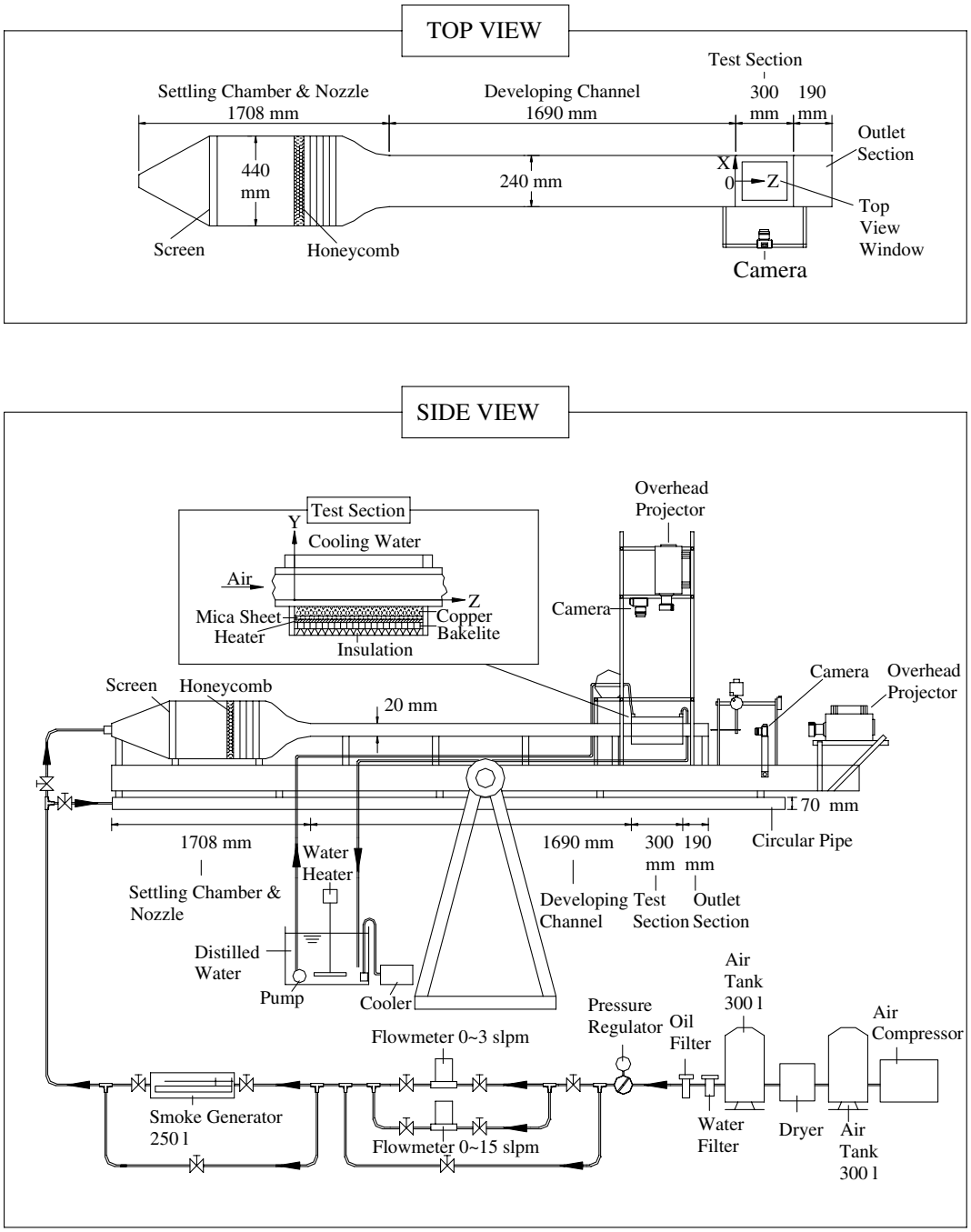

Fig. 1. Schematic of experimental apparatus and the chosen coordinate system for the test section.

oscillations are measured at selected detection points. The sampling rate of the data channel in the data acquisition unit is set at 0.08 s per scan which is much shorter than the period of the flow oscillation in the low Reynolds number mixed convective flow considered here.

Visualization of the buoyancy driven vortex flow in the test section is realized by injecting smoke tracers at some distance ahead of the settling chamber. By using a 1.5–2.5 mm plane light sheet from an overhead projector with an adjustable knife edge to illuminate the flow field containing these smoke particles, a sharp contrast could be achieved between the duct walls and smoke. Then the flow photos from the top, side and end views of the test section can be taken.

2.2. Mounting the block and experimental procedures

A rectangular block made of acrylic, which has low thermal conductivity and diffusivity ($k = 0.16$ W/m k and $\alpha = 1.7 \times 10^{-7}$ m^2/s), is inserted from the outlet of the test loop into the duct and is placed directly on the bottom of the test section at the designated location. The size and shape of the two blocks as well as the chosen locations to be tested here are schematically shown in Fig. 2. Note that

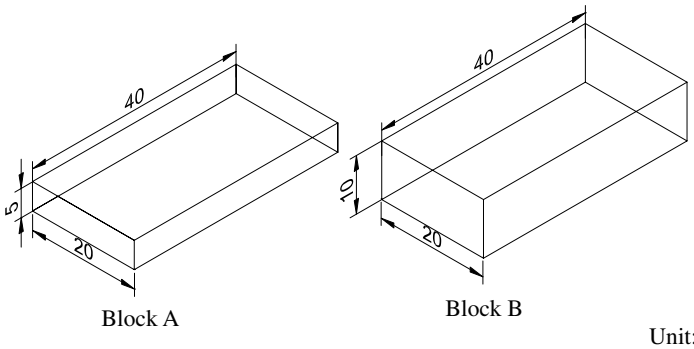

(a) Geometric size and shape

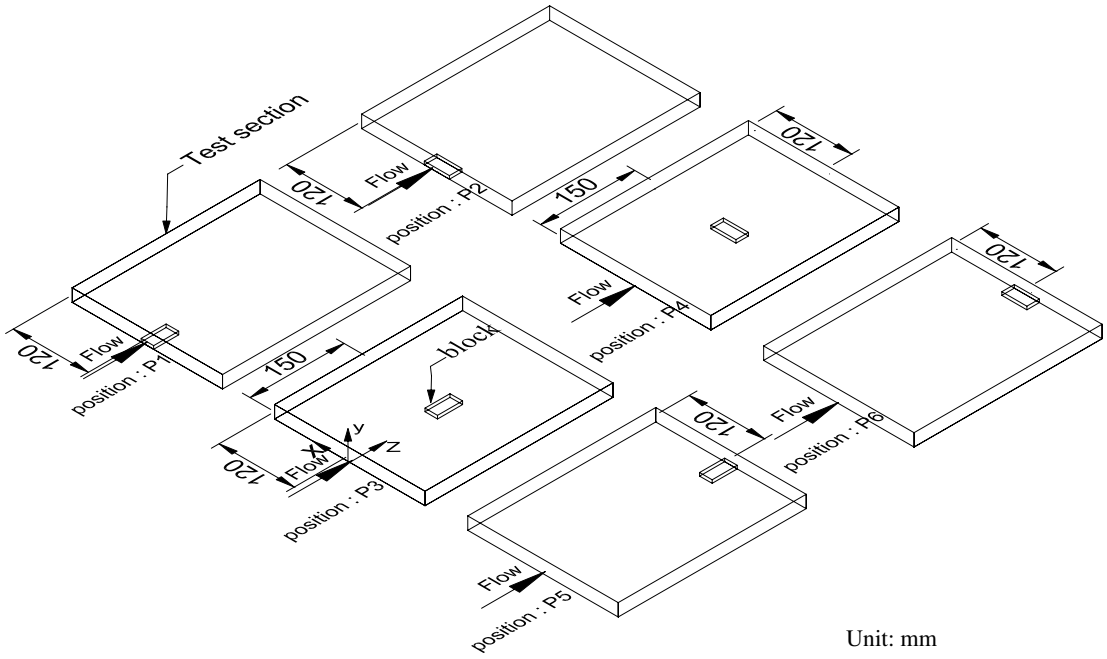

(b) Positions

Fig. 2. Geometric size and shape (a) and positions of the mounted blocks (b).

the height of block B is twice of block A. Besides, at a given location the long or short sides of the blocks can be placed normal to the forced flow direction. These two different orientations of the blocks are expected to exert very different influences on the vortex flow patterns. The surfaces of the blocks are polished to become rather smooth in order to minimize the possible disturbances to the vortex flow from the surface roughness. Note that the forced air flow and the buoyancy driven natural convection flow considered here are both at relatively low speed in the flat duct and hence the block cannot be shaken or moved by the air flow in the test. In this study the blocks are placed at three different locations with their geometric centers all along the longitudinal centerline of the duct bottom, as indicated in Fig. 2. According to the location and orientation of a given block, we have six different positions of the block in the test. They are designated as positions P_1–P_6 indicated in Fig. 2.

In each experiment the air compressor, dryer, DC power supplies, and the distilled water unit are turned on first and set at the predetermined levels. Meanwhile, the distilled water is circulated over the top plate and the top and bottom plates are controlled at the preset temperatures. Then all the experimental parameters are checked and recorded by the data acquisition unit. Usually, it takes about 3 h for the Rayleigh number and the distilled water temperature to be raised to the test point, and another 2 h are needed to maintain the vortex flow at the stable or statistical state. Finally we start the temperature measurement and flow visualization.

2.3. Analysis of data uncertainty

Uncertainties in the Rayleigh number, Reynolds number and other independent parameters are calculated

according to the standard procedures established by Kline and McClintock [28]. The uncertainties of the thermophysical properties of air are included in the analysis. The fundamental thermophysical properties of the working fluid (air) are $\alpha = 0.220$ (cm^2/s), $\beta = 0.00335$ (1/K), $Pr = 0.737$ and $v = 0.162$ (cm^2/s) at 30 °C and 0.997 bar. The fluid properties are real time corrected based on the temperature and pressure detected at the inlet of the test section. In addition, the uncertainties of the control unsteadiness and temperature non-uniformities on the top and bottom plates are accounted for in the evaluation of the data uncertainty. The analysis shows that the uncertainties of temperature,

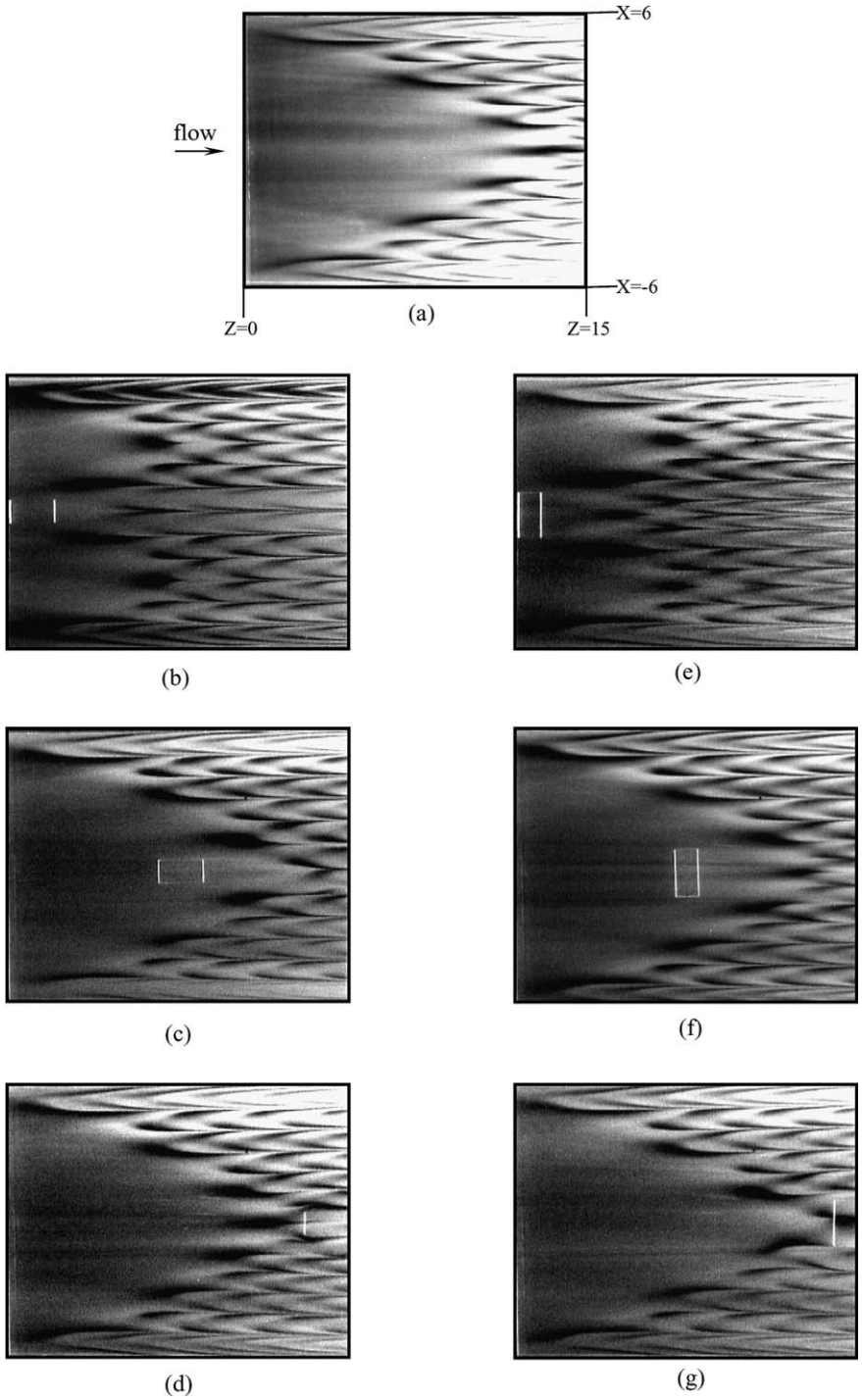

Fig. 3. Top view flow photos taken at mid-height of the duct for (a) without block, (b) block A located at P_1, (c) block A located at P_3, (d) block A located at P_5, (e) block A located at P_2, (f) block A located at P_4, and (g) block A located at P_6, showing the effects of the block location and orientation on longitudinal rolls for $Ra = 6003$ at $Re = 30.0$ ($Gr/Re^2 = 9.4$).

volume flow rate, dimensions, Reynolds number and Rayleigh number measurements are estimated to be ±0.15 °C, ±1%, ±0.005 mm, ±2% and ±5%, respectively.

3. Results and discussion

Selected results from the present flow visualization and temperature measurement are presented in the following to illustrate how the presence of a wall-mounted rectangular block affects the vortex flow structures and their stability in the bottom heated horizontal flat duct over the range of the parameters covered here. Particular attention is paid to the effects of the block size, orientation and location on the longitudinal, transverse and mixed vortex flow patterns at long time when all the initial transients in the flow die out and the flow already reaches steady or statistical state.

3.1. Effects of block on longitudinal vortex flow

It is well known that at slightly supercritical buoyancy for the Reynolds number exceeding certain low value the resulting vortex flow in the unblocked duct at long time is in the form of steady longitudinal vortex rolls [1]. To illustrate the effects of the mounted block on this longitudinal vortex flow, the top view flow photos at steady or statistical state taken at the midheight of the duct ($y = 1/2$) with block A mounted at different locations and orientations are shown in Fig. 3 for $Re = 30.0$ and $Ra = 6003$ along with that for the unblocked duct. Since the votex rolls induced in the mixed convection flow considered here have the same diameter which is equal to the duct height, the top view flow photos taken at the mid-height of the duct are representative for that taken at other

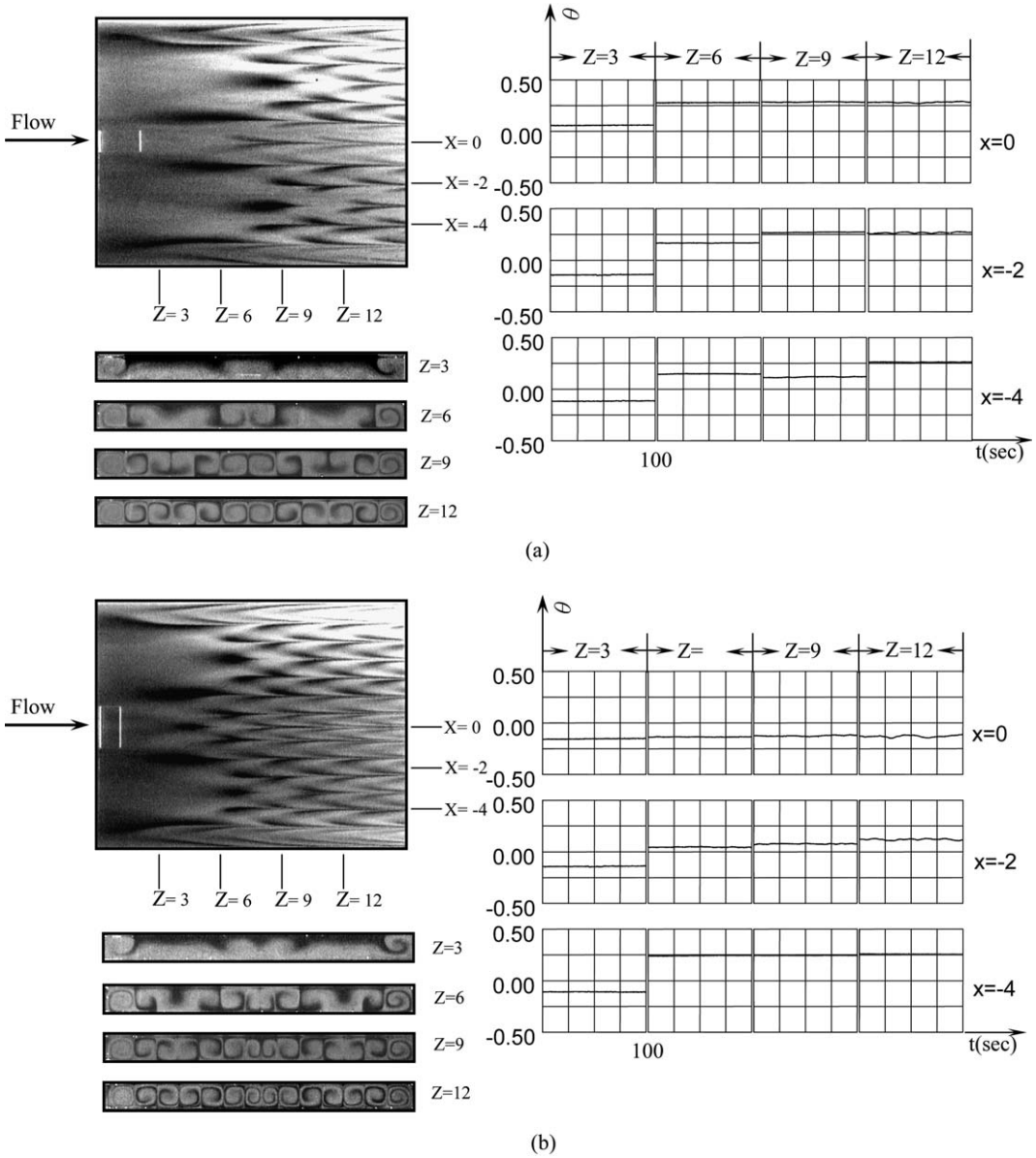

Fig. 4. Temporal structure of vortex flow revealed from top and end view flow photos at statistical state and time records of air temperature at selected locations at $y = 1/2$ and $x = 0$, -2 and -4 for block A mounted at (a) position P_1 and (b) position P_2 for $Ra = 5008$ at $Re = 30.0$ ($Gr/Re^2 = 7.8$).

horizontal planes. Hence only those photos taken at the mid-height are presented in this study. The short sides of the block are normal to the forced flow direction in Fig. 3(b)–(d), while the long sides of the block are normal to the forced flow direction in Fig. 3(e)–(g). A comparison of the results in Fig. 3(a) and (b) clearly indicates that the onset points of the longitudinal rolls move substantially upstream especially for the pair of longitudinal vortex rolls directly behind the block when the block is placed near the duct entry. When the block is placed near the geometric center and exit end of the duct, the effects of the block on the longitudinal tolls are much milder (Fig. 3(c) and

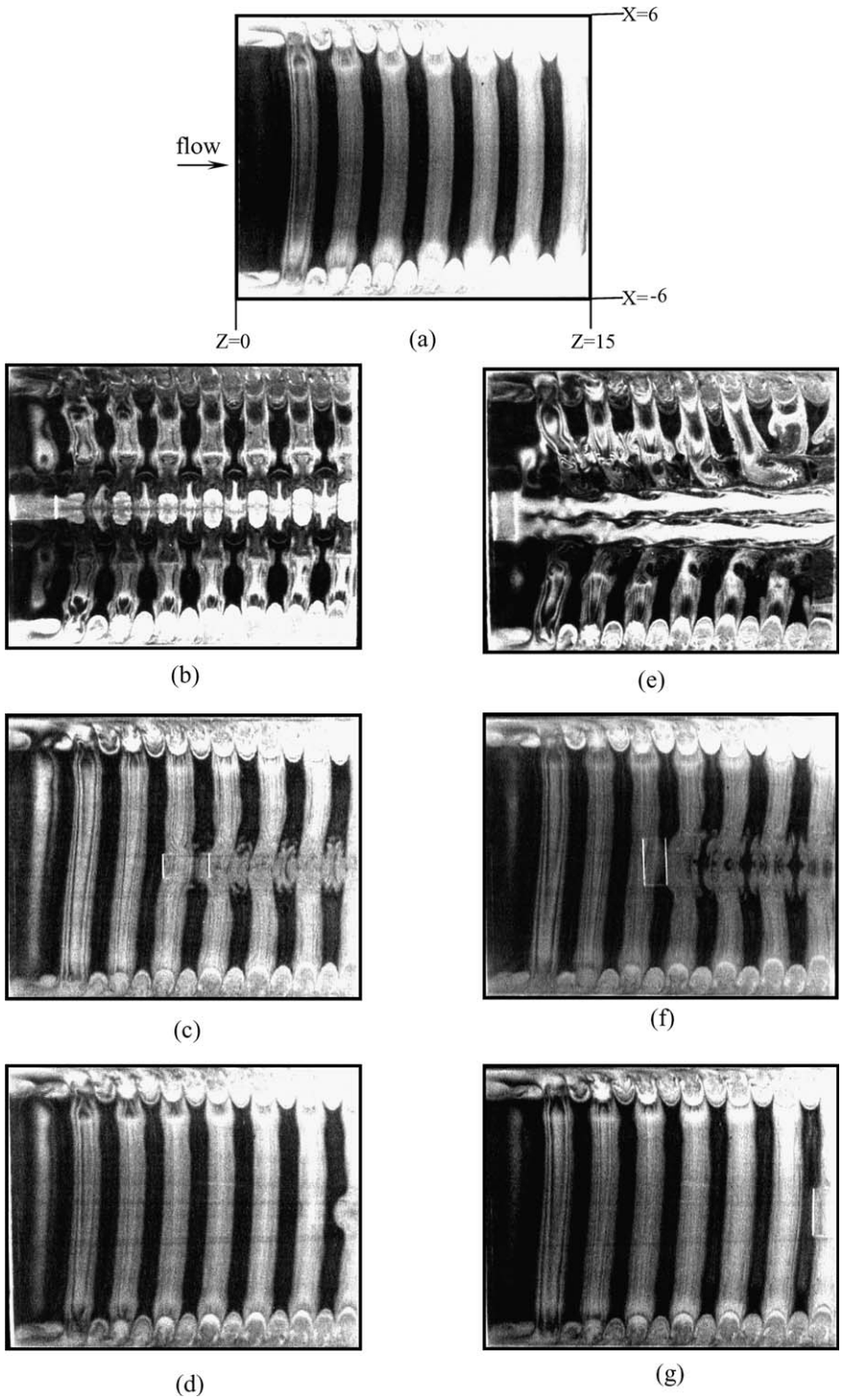

Fig. 5. Top view flow photos taken at mid-height of the duct for (a) without block, (b) block A located at P_1, (c) block A located at P_3, (d) block A located at P_5, (e) block A located at P_2, (f) block A located at P_4, and (g) block A located at P_6, showing the effects of the block location and orientation on transverse vortex flow for $Ra = 3007$ at $Re = 4.0$ ($Gr/Re^2 = 263.0$).

(d)). We move further to investigate how the orientation of the block affects of the longitudinal vortex flow by placing the block with its long sides normal to the forced flow direction. The associated results given in Fig. 3(e)–(g) again show that the longitudinal rolls appear at a much shorter distance from the duct inlet when the block is placed near the duct inlet. Besides, the vortex rolls directly behind the block are smaller in size and one more pair of vortex rolls are induced, compared to the unblocked duct. Note that the forced flow is blocked to a larger extent when the long sides of the block are normal to the forced flow direction. Hence this block orientation exhibits stronger effects on the vortex flow. Similar trend is noted for the effects of the block on the longitudinal vortex flow induced at different Rayleigh numbers.

To further manifest the effects of the block on the detailed characteristics of the longitudinal vortex flow, the top and end view flow photos along with the time records of the air temperature at selected locations for $Re = 30.0$ and $Ra = 5008$ are given in Fig. 4 for the block A placed near the duct inlet with its short and long sides respectively normal to the forced flow direction. In these plots and similar plots to be examined later the time $t = 0$ denotes an arbitrary time instant at steady or statistical state. The results in Fig. 4(a) show that for the short sides of the block normal to the forced flow direction, the longitudinal vortex flow is still spanwisely symmetric. But in the region near the duct exit and behind the block the flow is in a low amplitude oscillation with time, as clear from the time records at the locations $z = 12$ and $x = 0$ and -2. However, in the unblocked duct our previous study [1] indicates that the corresponding longitudinal vortex flow is steady in the entire duct. Now as the long sides of the block are normal to the forced flow direction (Fig. 4(b)), the unstable region of the longitudinal rolls is much larger by noting the temporal temperature oscillation at locations $z = 9$ and 12 and $x = 0$ and -2. Besides, the oscillation is stronger. Then, the effects of the block height on the longitudinal vortex flow are inspected by observing the top view flow photos at long time for blocks A and B placed at different locations and orientations. The results show that this change in the block height has very slight effects on the onset locations of the longitudinal rolls. Besides, for the block B the size of the longitudinal rolls directly behind the block is nearly the same as

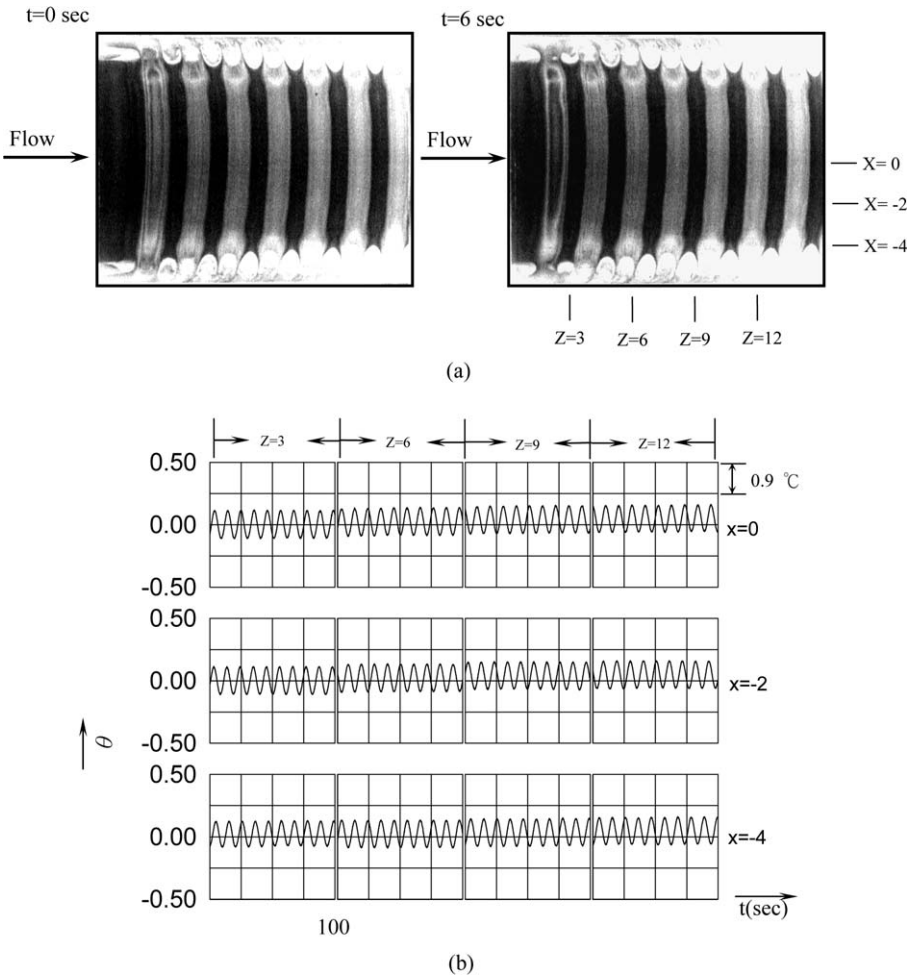

Fig. 6. Temporal structure of vortex flow revealed from (a) top view flow photos at statistical state and (b) time records of air temperature at selected locations at $y = 1/2$ and $x = 0$, -2, and -4 in the unblocked duct for $Ra = 3003$ at $Re = 4.0$ ($Gr/Re^2 = 263.0$, $t_p = 10.6$ s).

the other and we do not have an additional roll pair induced in the duct, unlike that for the block A. Finally, the destabilization of the longitudinal vortex flow in the exit portion of the duct can be slightly stronger due to the presence of block B.

In summary, placing the block near the duct inlet can cause the earlier onset of the longitudinal rolls especially in the region directly behind the block and can destabilize the longitudinal vortex flow in the exit portion of the duct again behind the block. Both effects are expected to promote the heat transfer in the flow. Moreover, with the long sides of block A normal to the forced flow direction an additional pair of longitudinal rolls can appear.

3.2. Effect of block on transverse vortex flow

The transverse vortex flow affected by block A mounted in two different orientations at various locations is illustrated in Fig. 5 by showing the top view photos at the statistical state for Re around 4.0 and $Ra = 3007$. When contrasted with the regular time periodic downstream moving transverse rolls prevailed in the unblocked channel (Fig. 5(a)), the results in Fig. 5(d) and (g) indicate that the transverse vortex flow is also little affected by the block placed near the duct exit. But when the block is placed in the middle section of the duct, the transverse rolls downstream of the block are slightly deformed (Fig. 5(c) and (f)). More specifically, the middle portion of the transverse rolls near the duct axis becomes somewhat distorted as they move over the block. The deformation of the transverse rolls as they move over the block can be more clearly seen from the corresponding side view flow photos at the central vertical plane ($x = 0$). The results show that near the block the cross-sections of the transverse rolls are highly distorted. As the transverse rolls move further downstream the roll distortion decays gradually. At the duct exit the

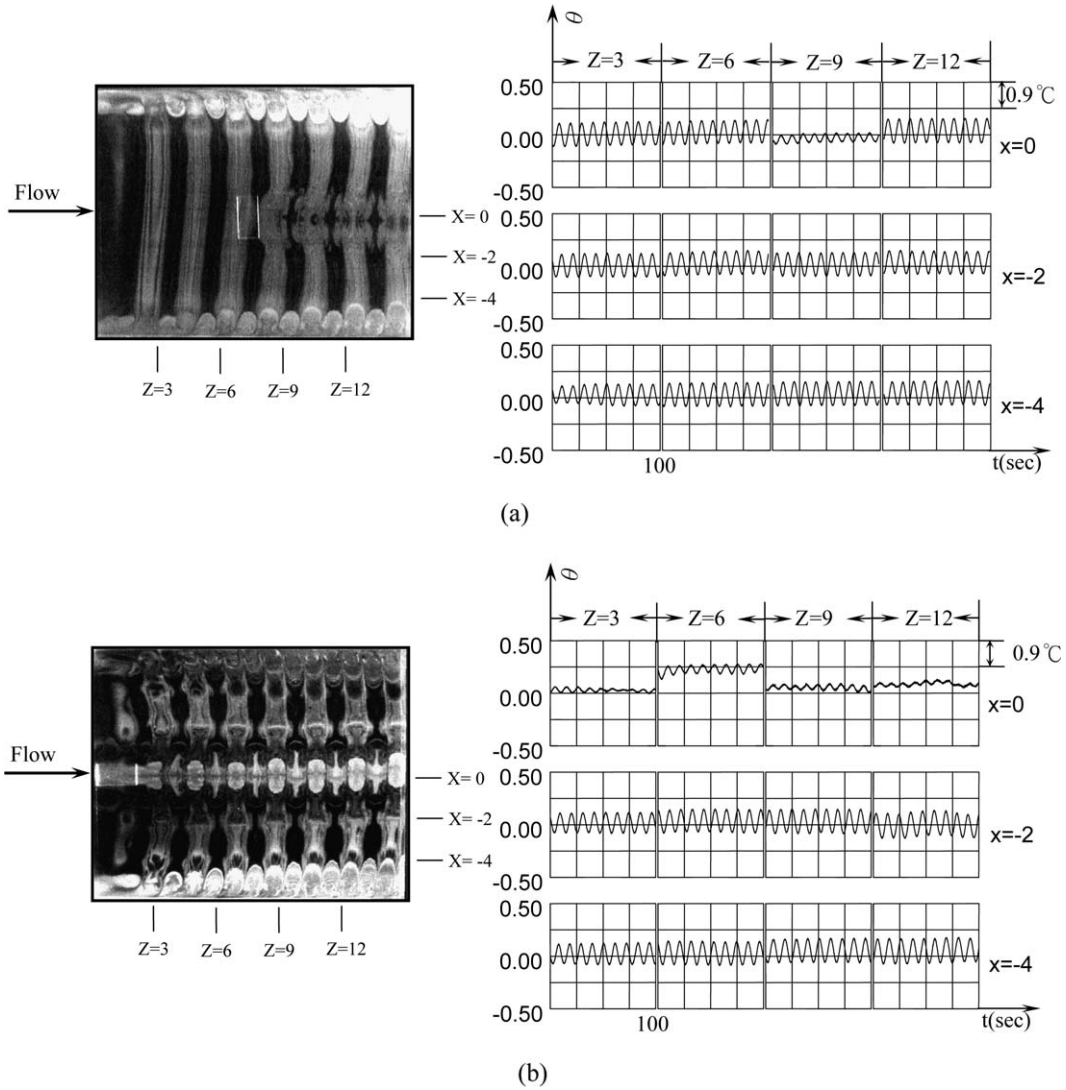

Fig. 7. Temporal structure of vortex flow revealed from top view flow photos at statistical state and time records of air temperature at selected locations at $y = 1/2$ and $x = 0$, -2 and -4 for block A mounted at (a) position P_4 and (b) position P_1 for $Ra = 3003$ at $Re = 4.0$ ($Gr/Re^2 = 263.0$, $t_p = 10.6$ s).

transverse rolls almost restore to their original regular shape. Now when the block is located near the duct inlet, significant distortion in the transverse vortex rolls is noted in Fig. 5(b) for the short sides of the block normal to the forced flow direction. The transverse rolls become sinuous to some extent and knotted as they just pass over the block. In the downstream the transverse rolls restore noticeably and become nearly straight in the spanwise direction, but they still contain knots. It is of interest to note that when the long sides of the block are normal to the forced flow direction (Fig. 5(e)), two deformed longitudinal rolls are induced right behind the block and extend to the duct exit. These two longitudinal rolls break the transverse rolls into two portions in the duct and cause them to become highly distorted.

The results for the transverse vortex flow with blocks A and B placed at different orientations and locations indicate that the block height exhibits much greater effects on the transverse rolls especially when the blocks are placed near the duct inlet. In particular, for block B with its height being twice of block A, a much larger region behind the block is dominated by the deformed longitudinal rolls when the long sides of the block are normal to the forced flow direction.

To reveal the effects of the block on the temporal characteristics of the transverse vortex flow, the time records of the air temperature at selected locations in the unblocked duct are examined first for the case presented above with $Re = 4.0$ and $Ra \approx 3000$. The experimental results given in Fig. 6 show that the entire flow oscillates at the same frequency ($t_p = 10.6$ s) and amplitude in the duct core where the fully developed transverse rolls prevail [1]. When block A is placed in the middle section of the duct, the results in Fig. 7(a) manifest that only in the small region right behind the block the flow oscillation is in a much smaller amplitude. Specifically, the reduction in the oscillation amplitude by the block presence is more than 50% by comparing the data in Figs. 6 and 7(a). Elsewhere the flow oscillates at nearly the same amplitude as that in the unblocked duct and the oscillation frequency of the flow is unaffected by the block. But

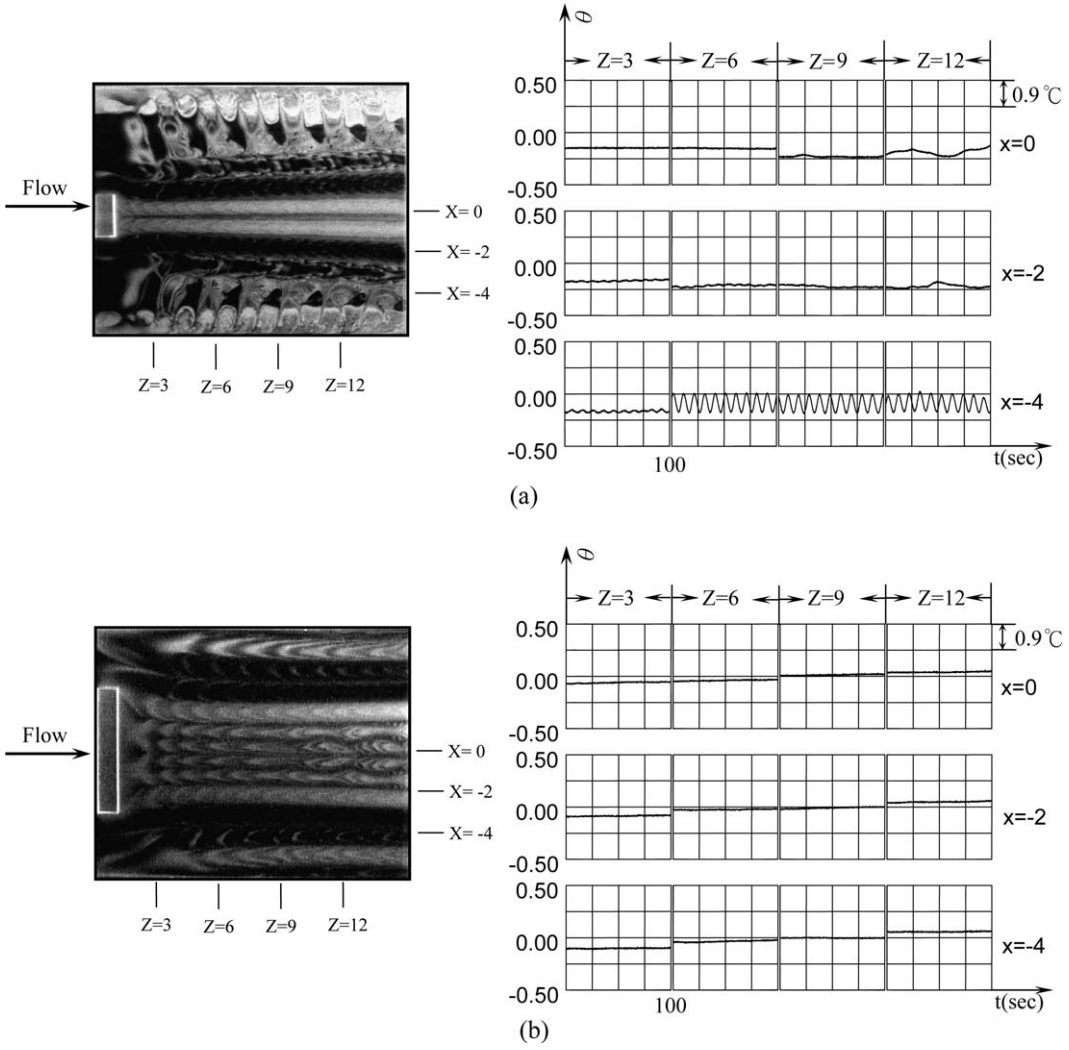

Fig. 8. Temporal structure of vortex flow revealed from top view flow photos at statistical state and time records of air temperature at selected locations at $y = 1/2$ and $x = 0$, -2 and -4 for (a) block B mounted at position P_2 for $Ra = 3002$ at $Re = 4.0$ ($Gr/Re^2 = 263.0$, $t_p = 10.6$ s), and (b) a longer block ($h = 12$ cm) mounted at position P_2 for $Ra = 3005$ at $Re = 4.0$ ($Gr/Re^2 = 263.0$).

when block A is mounted near the duct inlet, the flow oscillation is significantly suppressed in the entire downstream region behind the block (Fig. 7(b)). Note that the oscillation amplitude is also reduced by more than 50% in this region. Moreover, some irregularity in the temperature oscillation appears there. Outside this region the flow again oscillates at the same frequency as the unblocked duct.

Finally, the flow oscillation affected by block B is inspected. These results resemble qualitatively with those in Fig. 7 for block A. More specifically, the increase in the block height causes the flow in the small region right behind block B to become essentially steady, as evident from the time records of the air temperature at $z = 3$ and 6 and $x = 0$ given in Fig. 8(a). But in the region near the duct exit large amplitude, irregular flow oscillation appears. Slightly less effective flow stabilization by mounting block B on the duct bottom with its short sides normal to the forced flow direction is also noted. Moreover, it is of interest to note from the results in Fig. 8(b) that placing an even longer block of 12-cm in length, 1-cm in height and 2-cm in width in the duct entry with its long sides normal to the flow direction can completely suppress the temporal flow oscillation in the duct. However, weak and somewhat deformed longitudinal rolls still appear in the duct.

3.3. Effects of block on mixed vortex flow

Finally, how the mixed longitudinal and transverse vortex flow is affected by the mounted block is examined. The results for block A with the long sides of the block normal to the forced flow direction for $Re = 10.0$ and $Ra = 6002$ suggest that the effects of the block on the mixed vortex flow get stronger when the block is mounted at the more upstream location, similar to its effects on the longitudinal and the transverse vortex flows already discussed above. Behind the block, the flow again deforms substantially. And when the block is placed near the duct inlet, the transverse rolls in the duct core for the unblocked duct are trans-

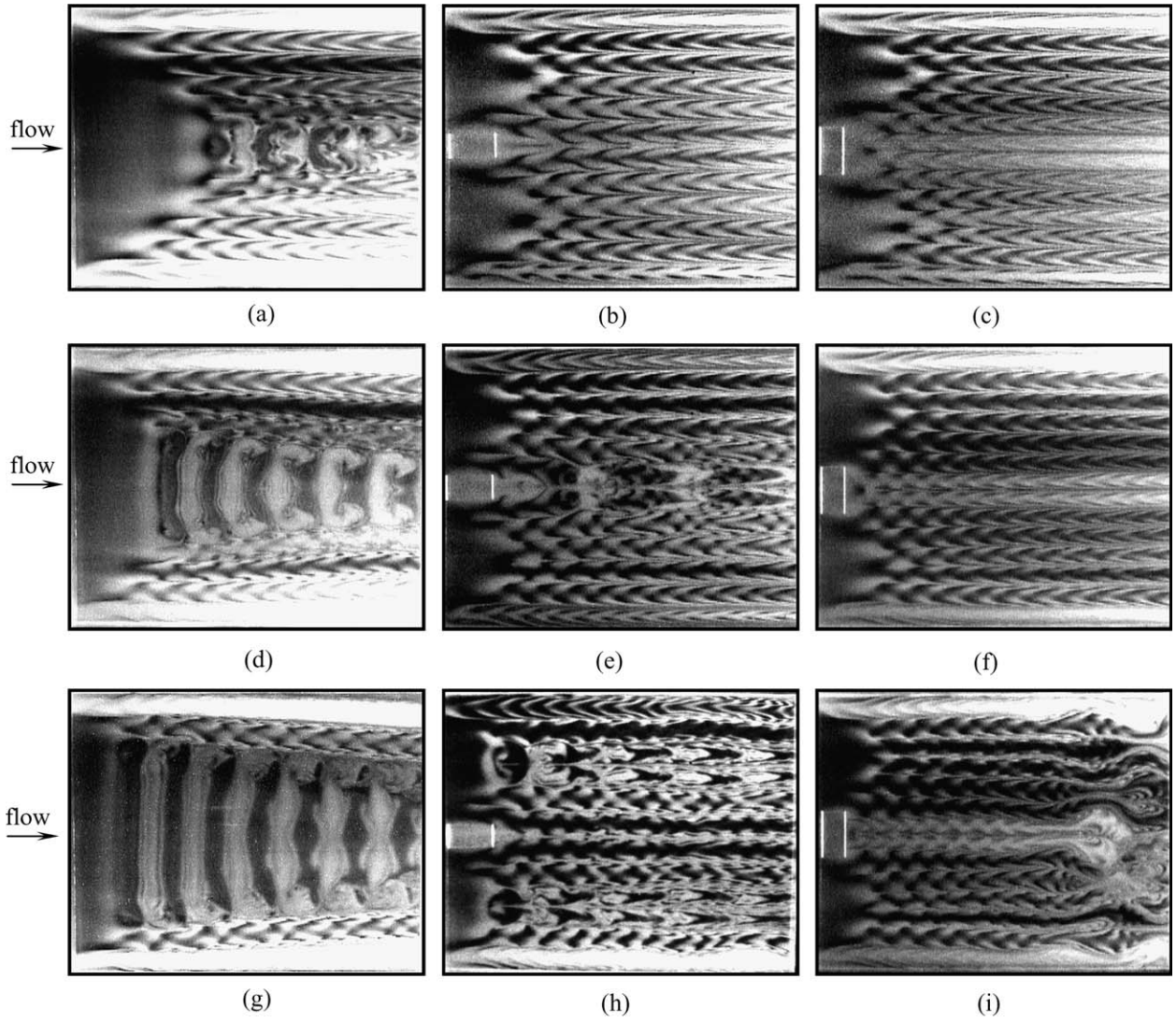

Fig. 9. Top view flow photos showing the effects of block A mounted at positions P_1 and P_2 on the mixed vortex flow for (a), (b) and (c) $Ra = 4003$ and $Re = 10.0$ ($Gr/Re^2 = 56.1$), for (d), (e) and (f) $Ra = 5005$ and $Re = 10.0$ ($Gr/Re^2 = 70.2$), and for (g), (h) and (i) $Ra = 6003$ and $Re = 10.0$ ($Gr/Re^2 = 84.2$).

formed to the longitudinal rolls. But these longitudinal rolls are somewhat unstable and they become highly deformed in the exit half of the duct. It is of interest to illustrate the influences of the block orientation, when block A is placed near the duct inlet, on the mixed vortex flow prevailed at different buoyancy-to-inertia ratios for $Re = 10.0$ in Fig. 9. The results in Fig. 9(a) and (b) indicate that at a low buoyancy-to-inertia ratio the transverse rolls only exist in a small portion of the unblocked duct and they all change to steady regular longitudinal rolls due to the presence of the block with its short sides normal to the forced flow direction. At a slightly higher buoyancy the transverse rolls occupy a larger portion of the unblocked duct (Fig. 9(d)) and they are changed to slightly deformed longitudinal rolls (Fig. 9(e)) by the presence of the block. The corresponding time records of the air temperature indicate that the flow oscillation is significantly suppressed by the block as the transverse rolls are changed to the longitudinal rolls behind the block. But near the duct exit large amplitude, irregular flow oscillation begins to appear. At an even higher buoyancy-to-inertia ratio the block causes the vortex flow downstream of it to become somewhat irregular (Fig. 9(h)). The associated time records of the air temperature given in Fig. 10(a) again show the suppression of the flow oscillation by the block presence, and in the exit half of the duct the flow oscillation is intense and irregular. Now when block A is placed near the duct inlet with its long sides normal to the flow direction, the mixed vortex flow is changed to regular longitudinal vortex flow (Fig. 9(c) and (f)) except at the relatively high buoyancy-to-inertia ratio (Fig. 9(i)). At such high buoyancy-to-inertia ratio the longitudinal vortex rolls are unstable and highly deformed in the exit portion of the blocked duct. The corresponding flow oscillation shown in

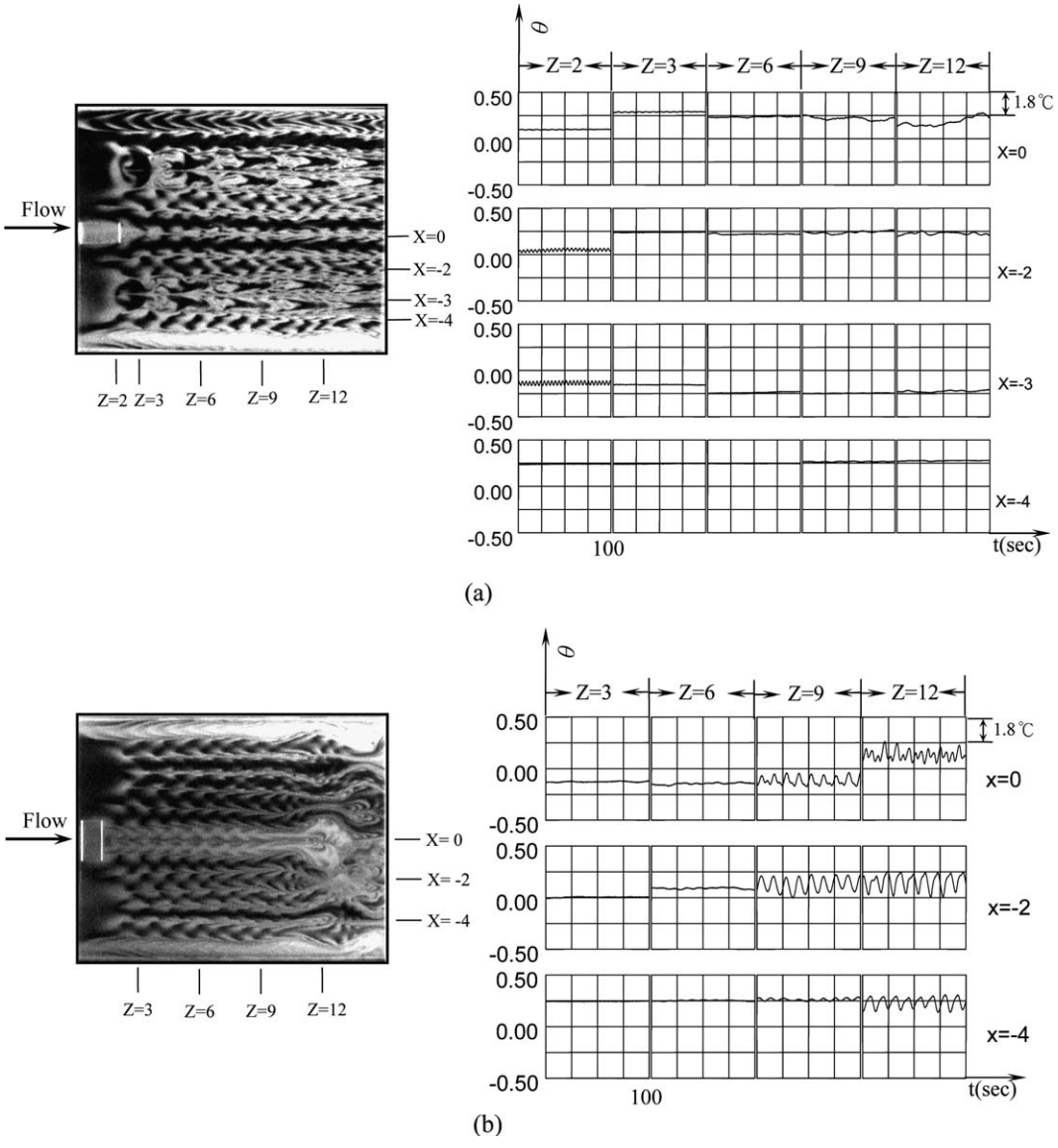

Fig. 10. Temporal structure of vortex flow revealed from top view flow photos at statistical state and time records of air temperature at selected locations at $y = 1/2$ for block A mounted at (a) position P_1 and (b) position P_2 for $Ra = 6002$ at $Re = 10.0$ ($Gr/Re^2 = 84.2$).

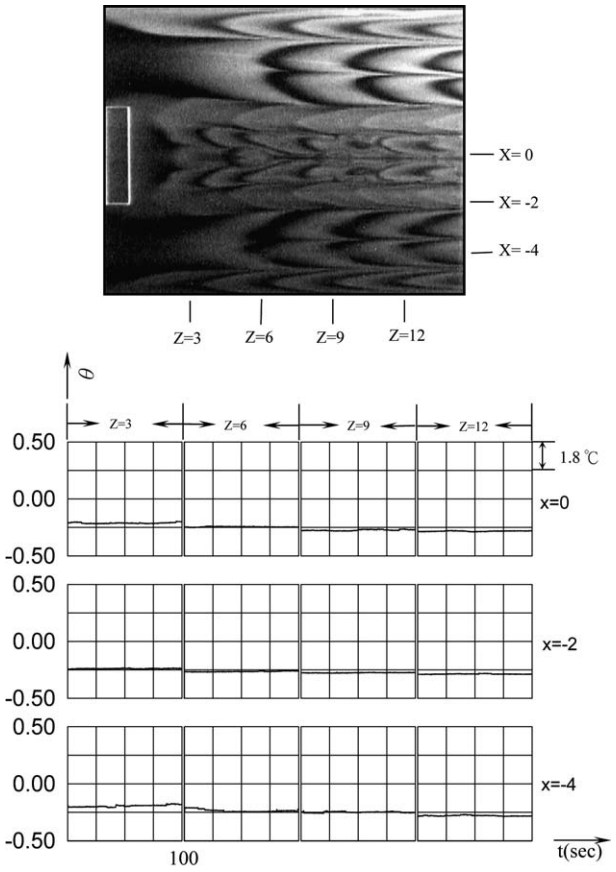

Fig. 11. Temporal structure of vortex flow revealed from top view flow photo at statistical state and time records of air temperature at selected locations at $y = 1/2$ and $x = 0$, -2 and -4 for a longer block ($h = 8$ cm) mounted at position P_2 for $Ra = 6008$ at $Re = 10.0$ ($Gr/Re^2 = 84.2$).

Fig. 10(b) is nearly time periodic and in a large amplitude in this portion of the duct. Moreover, it is noted that by mounting a longer block of 8-cm in length, 1-cm in height and 2-cm in width the temporal flow oscillation can be almost completely suppressed in the duct (Fig. 11).

To further illustrate the effects of the block height on the mixed vortex flow, the top view flow photos affected by blocks A and B placed near the duct inlet with two different orientations are compared for $Re = 10.0$ and $Ra = 4002$, 5004 and 6008. A close inspection of these results reveals that the regularization of the vortex flow by block B with a larger height is much more prominent. Specifically, steady longitudinal vortex flow prevails in the duct when block B is mounted near the duct inlet for all cases examined here except for $Re = 10.0$ and $Ra = 6008$ in which some flow deformation is noted.

4. Concluding remarks

Experimental flow visualization and transient temperature measurement have been carried out in the present study to explore how a wall-mounted rectangular block affects the vortex flow structure in mixed convection of air through a bottom heated horizontal flat duct. Two acrylic blocks with different heights were mainly tested here. The effects of the block orientation and length are also examined. Each mounted block was placed along the longitudinal centerline of the duct bottom, and the Reynolds and Rayleigh numbers of the flow were respectively varied from 3 to 30 and 3000 to 6000 in the experiment. The major results obtained can be summarized in following:

(1) In the ranges of the Reynolds and Rayleigh numbers at which the longitudinal vortex flow prevails in the unblocked duct, placing block A or B near the duct entry causes earlier onset of the longitudinal rolls especially in the region directly behind the block and can destabilize the longitudinal vortex flow in the exit portion of the duct. When the block is mounted in the exit half of the duct, the longitudinal vortex flow is only slightly affected.

(2) The transverse vortex flow is also slightly affected by the block when it is placed near the duct exit or the geometric center of the duct bottom. However, the transverse rolls deform significantly as they pass over the block. Meanwhile the air temperature oscillation is in much smaller amplitude in the region behind the block. Elsewhere the flow is also time periodic and oscillates at nearly the same frequency and amplitude as that in the unblocked duct. When block A is placed near the duct inlet the transverse rolls downstream of the block become sinuous and knotted for the short sides of the block normal to the forced flow direction. But when the long sides of the block are normal to the forced flow direction, two deformed longitudinal rolls appear in the region behind the block and the transverse rolls are splitted into two portions and are somewhat distorted. Increasing the block height can regularize the longitudinal rolls. Suppression of the flow oscillation by the block is significant in the region behind the block. The flow behind block B can be completely stabilized. A further increase of the block length can completely stabilize the temporal flow oscillation in the duct.

(3) For the mixed vortex flow in the unblocked duct, the transverse rolls in the duct core can be significantly affected by the mounted block. The longitudinal rolls near the duct sides are less affected. Specifically, placing block A near the duct inlet can change the transverse rolls to regular or deformed longitudinal rolls depending on the buoyancy-to-inertia ratio and orientation of the block. Flow stabilization by the block is prominent. More effective flow stabilization can be obtained by increasing the block height and placing the block with its long sides normal to the forced flow direction. Flow behind block B is essentially steady except in the exit portion of the duct. Moreover, a longer block can suppress nearly all the temporal flow oscillation in the duct.

During the course of this investigation, it is realized that the transverse and mixed vortex flows can be partially stabilized by placing block A or B near the duct inlet. Specifically, in the region behind the block the vortex flow can be stabilized. Increasing the block height can produce more profound flow stabilization effects in a larger region. We need to systematically explore how the length, width, height and even the shape of the block affect the stability of the vortex flows. This needs to be investigated in the near future.

Acknowledgement

The financial support of this study by the engineering division of National Science Council of Taiwan, ROC through the NSC83 0404 E009 054 is greatly appreciated.

References

[1] C.H. Yu, M.Y. Chang, T.F. Lin, Structures of moving transverse and mixed rolls in mixed convection in a horizontal plane channel, Int. J. Heat Mass Transfer 40 (1996) 333–346.
[2] F.P. Incropera, Convective heat transfer in electronic equipment cooling, ASME. J. Heat Transfer 100 (1988) 1097–1111.
[3] M.L. Hitchman, K.F. Jensen, Chemical vapor deposition (principle and application), 1993, 245–381 (Chapter 6).
[4] W.S. Tseng, W.L. Lin, C.P. Yin, C.L. Lin, T.F. Lin, Stabilization of buoyancy driven unstable vortex flow in mixed convection of air in a rectangular duct by tapering its top plate, ASME. J. Heat Transfer 122 (2000) 58–65.
[5] Y. Mori, Y. Uchida, Forced convective heat transfer between horizontal flat plates, Int. J. Heat Mass Transfer 9 (1966) 803–817.
[6] M. Akiyama, G.J. Hwang, K.C. Cheng, Experiments on the onset of longitudinal vortices in laminar forced convection between horizontal plates, ASME. J. Heat Transfer 93 (4) (1971) 335–341.
[7] S. Ostrach, Y. Kamotani, Heat transfer augmentation in laminar fully developed channel flow by means of heating from below, ASME. J. Heat Transfer 97 (1975) 220–225.
[8] Y. Kamotani, S. Ostrach, Effect of thermal instability on thermally developing laminar channel flow, ASME. J. Heat Transfer 98 (1976) 62–66.
[9] G.J. Hwang, C.L. Liu, An experimental study of convective instability in the thermal entrance region of a horizontal parallel-plate channel heated from below, Can. J. Chem. Eng. 54 (1976) 521–525.
[10] F.P. Incropera, A.L. Knox, J.R. Maughan, Mixed-convection flow and heat transfer in the entrance region of a horizontal rectangular duct, ASME. J. Heat Transfer 109 (1987) 434–439.
[11] J.R. Maughan, F.P. Incropera, Regions of heat transfer enhancement for laminar mixed convection in a parallel plate channel, Int. J. Heat Mass Transfer 33 (1990) 555–570.
[12] S.S. Moharreri, B.F. Armaly, T.S. Chen, Measurements in the transition vortex flow regime of mixed convection above a horizontal heated plate, ASME. J. Heat Transfer 110 (1988) 358–365.
[13] K.C. Chiu, F. Rosenberger, Mixed convection between horizontal plate-I. Entrance effects, Int. J. Heat Mass Transfer 30 (1987) 1645–1654.
[14] K.C. Chiu, J. Ouazzani, F. Rosenberger, Mixed convection between horizontal plate-II. Fully developed flow, Int. J. Heat Mass Transfer 30 (1987) 1655–1662.
[15] T.A. Nyce, J. Ouazzani, A. Durand-Daubin, F. Rosenberger, Mixed convection in a horizontal rectangular channel-experimental and numerical velocity distributions, Int. J. Heat Mass Transfer 35 (1992) 1481–1494.
[16] M.T. Ouazzani, J.P. Caltagirone, G. Meyer, A. Mojtabi, Etude numérique et expérimentale de la convection mixte entre deux plans horizontaux à températures différences, Int. J. Heat Mass Transfer 32 (1989) 261–269.
[17] M.T. Ouazzani, J.K. Platten, A. Mojtabi, Etude expérimentale de la convection mixte entre deux plans horizontaux à températures différences-II, Int. J. Heat Mass Transfer 33 (1990) 1417–1427.
[18] K.C. Cheng, L. Shi, Visualization of convective instability phenomena in entrance region of a horizontal rectangular channel heated from below and/or cooled from above, Exp. Heat Transfer 7 (1994) 235–248.
[19] H. Koizumi, L. Hosokawa, Unsteady behavior and mass transfer performance of combined convective flow in a horizontal rectangular duct heated from below, Int. J. Heat Mass Transfer 36 (1993) 3937–3947.
[20] M.K. Chyu, V. Natarajan, Local heat/mass transfer distributions on the surface of a wall-mounted cube, ASME. J. Heat Transfer 113 (1991) 851–857.
[21] T. Igarashi, Fluid flow and heat transfer around rectangular cylinders (the case of a width/height ratio of a diction 0.33–1.5), Int. J. Heat Mass Transfer 30 (5) (1987) 893–901.
[22] S.S. Hsieh, H.J. Shih, Y.J. Hong, Laminar forced convection from surface-mounted ribs, Int. J. Heat Mass Transfer 33 (1990) 1987–1999.
[23] T. Igarashi, Heat transfer from a square prism to an air stream, Int. J. Heat Mass Transfer 28 (1) (1985) 171–181.
[24] M.K. Chyu, V. Natarajan, Heat Transfer on the base surface of three-dimensional protruding elements, Int. J. Heat Mass Transfer 39 (14) (1996) 2925–2935.
[25] J.C. Han, J.S. Park, C.K. Lei, Heat transfer enhancement in channels with turbulence promoters, ASME. J. Heat Transfer 107 (1985) 628–635.
[26] J.C. Han, Heat transfer and friction characteristics in rectangular channels with rib turbulators, ASME. J. Heat Transfer 110 (1988) 321–328.
[27] M.Y. Chang, C.H. Yu, T.F. Lin, Flow visualization and numerical simulation of transverse and mixed vortex roll formation in mixed convection of air in a horizontal flat duct, Int. J. Heat Mass Transfer 40 (1997) 1907–1922.
[28] S.J. Kline, F.A. McClintock, Describing uncertainties in single-sample experiments, Mech. Eng. 75 (1953) 3–12.